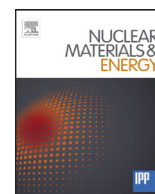




Contents lists available at ScienceDirect

## Nuclear Materials and Energy

journal homepage: [www.elsevier.com/locate/nme](http://www.elsevier.com/locate/nme)

## Effect of impurity deposition layer formation on D retention in LHD plasma exposed W

Y. Oya<sup>a,\*</sup>, H. Fujita<sup>a</sup>, C. Hu<sup>a</sup>, Y. Uemura<sup>a</sup>, S. Sakurada<sup>a</sup>, K. Yuyama<sup>a</sup>, X. Li<sup>a</sup>, Y. Hatano<sup>b</sup>,  
N. Yoshida<sup>c</sup>, H. Watanabe<sup>c</sup>, Y. Nobuta<sup>d</sup>, Y. Yamauchi<sup>d</sup>, M. Tokitani<sup>e,f</sup>, S. Masuzaki<sup>e</sup>,  
T. Chikada<sup>a</sup>

<sup>a</sup> Graduate School of Science, Shizuoka University, Shizuoka, Japan<sup>b</sup> Hydrogen Isotope Research Center, Organization for Promotion of Research, University of Toyama, Toyama, Japan<sup>c</sup> Institute for Applied Mechanics, Kyushu University, Kasuga, Fukuoka, Japan<sup>d</sup> Graduate School of Engineering, Hokkaido University, Sapporo, Japan<sup>e</sup> Department of Helical Plasma Research, National Institute for Fusion Science, Toki, Japan<sup>f</sup> SOKENDAI (Grad. University for Advanced Studies), 322-6 Oroshi-cho, Toki 509-5292, Japan

## ARTICLE INFO

## Article history:

Received 10 November 2015

Revised 6 April 2016

Accepted 1 July 2016

Available online xxx

## Keywords:

Hydrogen isotope retention enhancement

Mixed-material layer

TEM

TDS

XPS

LHD

## ABSTRACT

Effect of carbon based mixed-material deposition layer formation on hydrogen isotope retention was studied. The tungsten (W) samples were placed at four different positions, namely PI (sputtering erosion dominated area), DP (deposition dominated area), HL (higher heat load area), and ER (erosion dominated area) during 2013 plasma experimental campaign in Large Helical Device (LHD) at National Institute for Fusion Science (NIFS), Japan and were exposed to ~ 4000 shots of hydrogen plasma in a 2013 plasma experimental campaign. Most of the sample surface except for ER was covered by a mixed-material deposition layer formed by plasma experimental campaign, which consisted of carbon, but some metal impurities were contained. For ER sample, He bubbles were formed due to long term He discharge cleaning and He plasma experiments during the plasma experimental campaign. The additional 1 keV D<sub>2</sub><sup>+</sup> implantation was performed to evaluated the D retention enhancement by plasma exposure. It was found that both of H and D retentions were clearly increased. In particular, the H retention was controlled by the thickness of the carbon-dominated mixed-material deposition layer, indicating most of the H was trapped by this mixed-material deposition layer. It is concluded that the accumulation of low-Z mixed-material layer on the surface of the first wall is one of key issues for the determination of hydrogen isotope retention in first wall.

© 2016 The Authors. Published by Elsevier Ltd.

This is an open access article under the CC BY-NC-ND license

(<http://creativecommons.org/licenses/by-nc-nd/4.0/>).

## 1. Introduction

Tungsten (W) is a candidate for plasma facing materials (PFMs) for future fusion reactors [1–2]. During the plasma discharge, various energetic particles will be implanted into W, leading to the introduction of irradiation damages. Recently, the damage concentration influence on hydrogen isotope retention in W was studied using heavy ion irradiation, and comparison of D retention for ion-damaged W and neutron irradiated W was performed. It can be said that damage distribution and density will be key parameters for hydrogen isotope trapping states [3–7]. On the other hand, it is thought that surface modification is caused by the change in the

surface chemical state by the reaction of tungsten with carbon, one of the major impurities. It is well known that the formation of W–C mixed layer will enhance the hydrogen isotope retention in PFMs during D–T fusion operation. It is also reported that the carbon retained in tungsten plays a role of diffusion barrier for hydrogen isotopes toward the bulk, resulting in the decrease of hydrogen isotope retention in W [8]. However, hydrogen isotopes will be accumulated in the carbon layer deposited on W surface. Several impurities such as carbon, oxygen were identified in the spherical tokamak (QUEST) although it was constructed with full metallic first walls [9].

Therefore, combination of damage introduction and impurity deposition would control the fuel retention in future fusion reactors, and knowledge related to fuel retention in the actual fusion reactor should be accumulated. In our previous studies in

\* Corresponding author.

E-mail address: [oya.yasuhisa@shizuoka.ac.jp](mailto:oya.yasuhisa@shizuoka.ac.jp) (Y. Oya).

Large Helical Device (LHD) at National Institute for Fusion Science (NIFS), the results of deuterium retention enhancement in the W samples exposed to the 2011 and 2012 plasma experimental campaign in LHD, respectively, were reported [10–12]. It was found that the accumulation of carbon based mixed-material deposition layer depended on the position on the plasma facing wall. In the deposition dominated area, more than 1  $\mu\text{m}$  thick mixed-material layer was formed. However, there are erosion dominant area, at which no deposition layer was found. The additional  $\text{D}_2^+$  implantation revealed that the shape of Thermal desorption spectroscopy (TDS) spectrum was clearly controlled by surface nature. Recently, closed divertor structure, which consists of graphite parts, was installed to enhance the plasma performance in LHD [13]. So, the concentration of carbon to stainless steel was increased year by year. In this study, the H retention in W placed in various positions during 2013 plasma experimental campaign in LHD was evaluated. The additional  $\text{D}_2^+$  implantation was also performed to evaluate the D trapping ability for plasma exposed W. These results were compared to the previous results exposed in 2012 experiment campaign and discuss the hydrogen isotope retention behavior with considering the experimental history.

## 2. Experimental setup

The mirror finished disk-type tungsten samples ( $\phi$  10 mm  $\times$  t 0.5 mm for TDS and  $\phi$  3 mm  $\times$  t  $\sim$  0.1 mm for Transmission Electron Microscopy (TEM)) was prepared by cutting polycrystalline tungsten rods manufactured by Allied Material Corp., Japan. All the samples were evacuated at 1173 K for 30 min in vacuum to remove residual hydrogen and damages introduced during fabrication processes. These samples were placed at four unique positions on the plasma facing wall in LHD, namely the higher plasma wall interaction area called the higher plasma wall interaction area (PI), the deposition area (DP), the higher heat load area (HL), and the erosion dominated area (ER). The detail positions are summarized in Fig. 1.

These samples were exposed to  $\sim$ 4600 hydrogen discharges during the 2013 experimental campaign, although there were  $\sim$ 5000 hydrogen discharges for the 2012 campaign. As shown in Fig. 1, the closed divertor structure, which consists of graphite parts, was installed in 9 sections to enhance the plasma performance [13]. The graphite surface area was increased about 1.4 times as large as that for the 2012 experimental campaign. During the plasma experimental campaign, long pulse He plasma discharges were performed and achieved steady-state plasma for maximum of 48 min in the 2013 campaign [14]. The sample temperature during the experimental campaign was less than 373 K. After the campaign, the samples were picked up and transported to Shizuoka University with air exposure. The 1.0 keV deuterium ions ( $\text{D}_2^+$ ) were additionally implanted into these samples ( $\phi$  10 mm  $\times$  t 0.5 mm) with the flux of  $1.0 \times 10^{18} \text{ D}^+ \text{ m}^{-2} \text{ s}^{-1}$  up to the fluence of  $5.0 \times 10^{21} \text{ D}^+ \text{ m}^{-2}$  to evaluate the enhancement of D retention capacity. The hydrogen isotope retention was estimated by TDS using two quadrupole mass spectrometers including high resolution mass spectrometer to distinguish  $\text{D}_2$  and He. The microstructure was observed by TEM using sample with size of  $\phi$  3 mm  $\times$  t  $\sim$  0.1 mm at Institute of Applied Mechanics, Kyushu University. The depth profiles of constituent atoms were evaluated by X-ray Photoelectron Spectroscopy (XPS) with combination usage of  $\text{Ar}^+$  sputtering technique.

## 3. Results and discussion

Fig. 2 show the surface morphologies for the samples placed at DP, PI, ER and HL positions observed by Scanning Electron Microscope (SEM). As mentioned in our last paper [12], most of

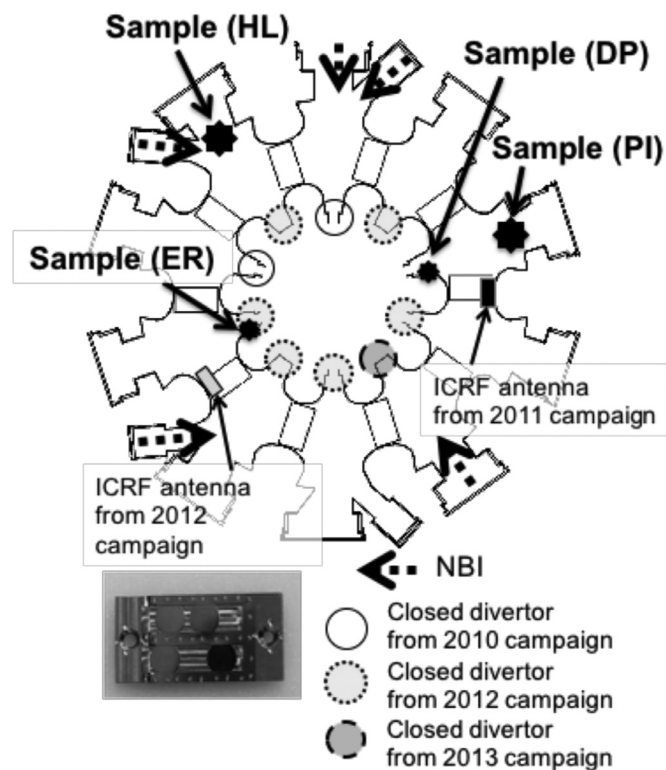


Fig. 1. Sample positions placed in LHD and history for introduction of closed divertor structure.

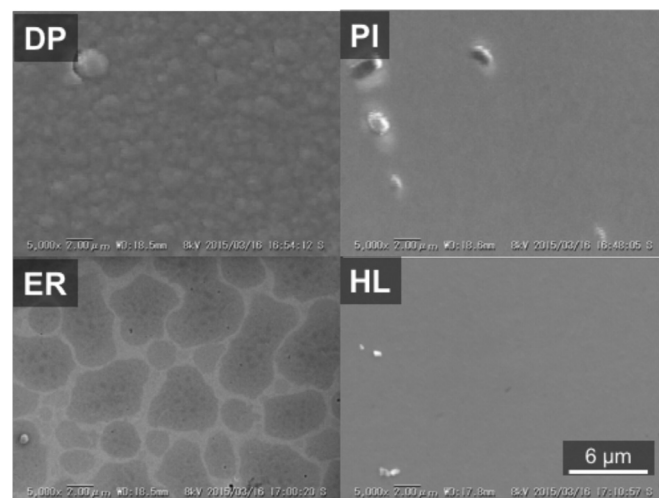


Fig. 2. SEM images of surface morphologies for W samples exposed to 2013 plasma experimental campaign.

the surface except for ER was deposition-dominated. However, even in erosion dominated regions, thin mixed-material layer can be found. The large imbricate deposits can be observed at the surface of the DP samples, leading to the formation of thicker deposition layer. For PI and HL samples, the surface was quite smooth, but some precipitates were adsorbed. The erosion trace like no deposition and sputtered trace, was found for ER samples and the morphology was quite different from the others. More detailed morphologies were observed by TEM as shown in Fig. 3. The formation of thicker mixed-material layer for DP sample prevents the ability to find the suitable position for TEM observation, but the clear amorphous carbon mixed material layers were formed for both of DP and PI samples. The small black dot reflecting

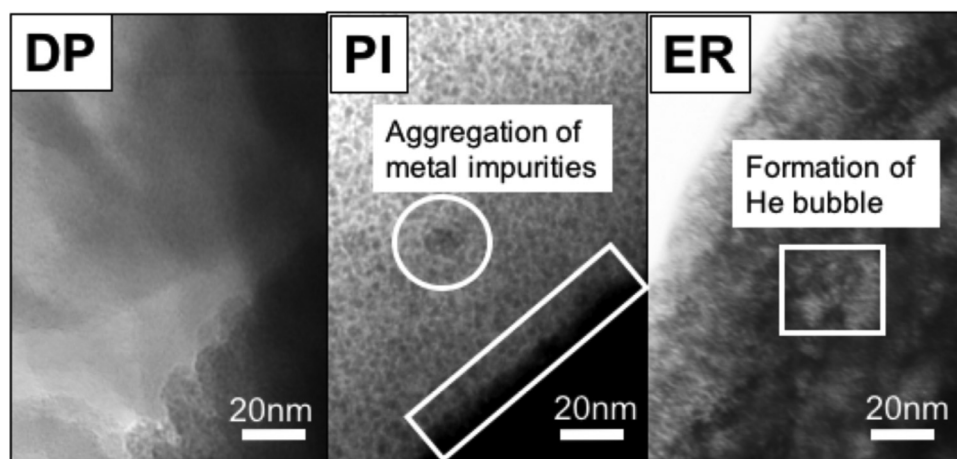


Fig. 3. TEM images of the mixed-material layer for DP, PI and ER samples exposed to 2013 experimental campaign.

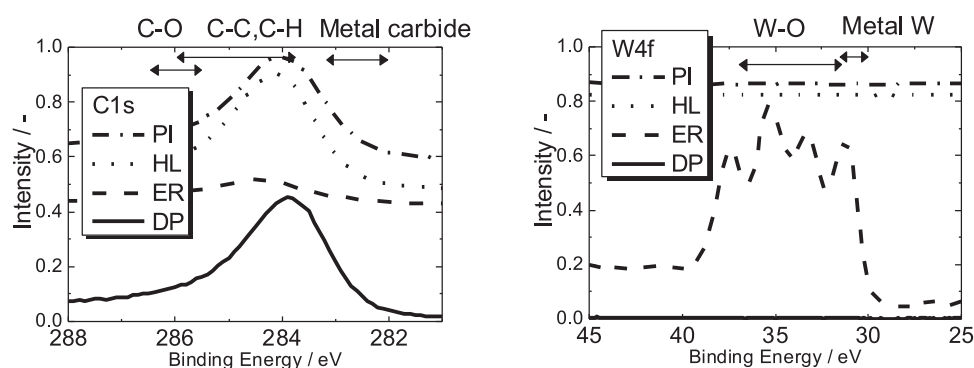


Fig. 4. C 1s and W 4f XPS spectra for the top surface of all the samples exposed to 2013 experimental campaign.

Table 1

Summary of atomic concentration for the top surface of all the samples exposed to 2013 experimental campaign.

	C	O	Cr	Fe	Ni	W
DP	94.0	4.7	0.0	0.2	0.0	0.0
PI	90.8	7.9	0.3	0.9	0.2	0.0
ER	31.7	39.0	0.0	0.1	0.1	23.4
HL	91.9	7.5	0.1	0.3	0.1	0.0

the existence of metal particles for TEM were widely distributed, which was almost the same as the previous experimental campaign [12]. In addition, the formation of He bubble was found for ER sample. In the 2013 experimental campaign, maximum of 48 min of long pulse He plasma discharge was performed, and other short and long pulse He discharges were conducted, which would induce He bubble formation.

The C 1s and W 4f XPS spectra for the top surface of all the samples exposed to the 2013 experimental campaign are shown in Fig. 4. The chemical state of carbon for all the samples except for ER sample was C–C or C–H bonds and no remarkable formation of metal carbide was found due to lower operation temperature during experimental campaign ( $<373$  K). According to W 4f XPS spectra, no existence of W was found except for ER sample. The chemical state of W for ER sample consisted of 2 states, namely metal W and W–O bond. Table 1 summarizes the atomic composition for the top surface of the samples after the 2013 experimental campaign. XPS analysis has no sensitivities for H and He, which were excluded in Table 1. The typical elements on the surface after the experimental campaign were carbon and oxygen, which were

the same as the previous experimental campaigns. But the carbon concentration was clearly increased compared to the previous campaigns of 81.8% (2012) and 79.3% (2011) at PI, 87.3% (2012) and 82.8% (2011) at HL [12]. This result can be explained that the divertor structure was changed from open divertor to closed divertor in the 9 sections, and the graphite surface area was increased about 1.4 times as large as that for the previous campaigns. Although the configuration near DP sample was still the open divertor, the carbon concentration also increased from 91.8% (2012) to 94%. This suggests that the carbon impurity would be transported from the other divertor areas. In addition, small amount of Fe, Cr, Ni which were the constituent atoms of stainless steel used for LHD first wall. These metals were contained in the carbon based mixed-material layer, which was consistent with TEM results. For ER sample, the carbon concentration is remarkably reduced and, concentrations of oxygen and tungsten was increased, indicating that tungsten oxide would be formed on the surface by energetic particle exposure (erosion dominated area). Fig. 5 shows the typical depth profile of atomic concentration for the DP sample evaluated by XPS with Ar<sup>+</sup> sputtering technique. The thickness of carbon based mixed-material deposition layer was 5  $\mu\text{m}$ . At the interface between mixed-material deposition layer and tungsten, oxygen concentration increased due to the formation of tungsten oxide.

These samples were picked up from LHD and additional 1.0 keV D<sub>2</sub><sup>+</sup> implantation with the fluence of  $5.0 \times 10^{21} \text{ D}^+ \text{ m}^{-2}$  was performed at Shizuoka University. Thereafter, H and D retentions were evaluated by TDS. Fig. 6 depicts H<sub>2</sub> and D<sub>2</sub> TDS spectra for D<sub>2</sub><sup>+</sup> implanted tungsten samples exposed to plasma discharges during the 2013 experimental campaign. For ER sample, the shape of TDS spectrum was quite different from the others. No large H<sub>2</sub> desorption was found and major D<sub>2</sub> desorption temperature was

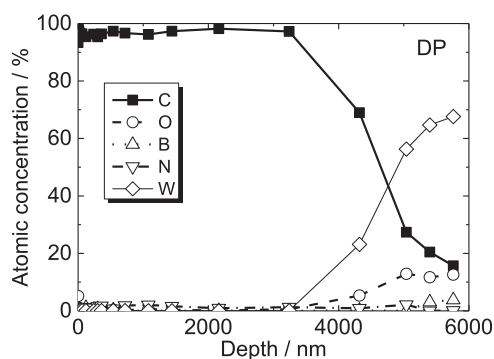


Fig. 5. Depth profile of atomic concentration for DP sample.

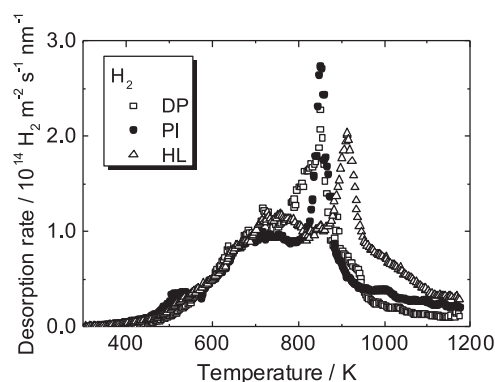


Fig. 7. H<sub>2</sub> TDS spectra normalized by thickness mixed material layer.

shifted toward lower temperature of 400 K and most of the D<sub>2</sub> was desorbed at the temperature less than 600 K, which was almost the same temperature region as the TDS spectrum for un-damaged W as shown in Fig. 6 [3]. Large H and D desorption was found for the DP sample, showing the large H retention and D trapping rate by additional D<sub>2</sub><sup>+</sup> irradiation. The major H<sub>2</sub> desorption temperature for the PI sample was located at lower temperature of less than 900 K, although that of D<sub>2</sub> was shifted toward higher temperature side at around 1000 K, indicating that some of H was replaced by D by D<sub>2</sub><sup>+</sup> implantation. As mentioned above from TEM observation, most of the sample surface except for ER sample was covered by carbon based mixed-material layer and the TDS spectra for these samples were quite different from that for W. Therefore, most hydrogen isotopes would be trapped by this mixed-material deposition layer and H<sub>2</sub> TDS spectra were normalized by their thicknesses as shown in Fig. 7. It was found that most of the H<sub>2</sub> desorption was almost the same, indicating that the major H was trapped by the carbon based mixed-material layer and the H retention would be controlled by the thickness of carbon based mixed-material layer. Table 2 summarizes the thicknesses of carbon based mixed-material deposition layer and, H & D retentions (desorbed as hydrogen gas form only) for all the samples. Note that H & D retentions for 2012 campaign mentioned in Ref. [12] were considered to include water desorption. But, in this paper, we have just focused on hydrogen gas desorption only, because desorption of water and hydrocarbon was found to be quite complex and it is difficult to distinguish them. The D trapping efficiency for the DP sample was much higher, indicating that the quick hydrogen isotope replacement may have occurred during D<sub>2</sub><sup>+</sup> implantation due to higher H retention. Most of H retentions for the samples exposed to 2013 experimental campaign were about two times as high as that exposed to the previous experimental campaign. In addition, the desorption of mass number of  $m/q = 14 \sim 20$  was also observed, but it was difficult to distinguish water and hydro-

carbons due to poor resolution of mass spectrometer. Therefore, contribution of water / hydrocarbons was not considered in this study. As can be found in Table 2, no large difference in the thickness of the mixed-material deposition layer was found between 2012 and 2013 experimental campaigns, although the number of shots to which they were exposed were  $\sim 5000$  shots and  $\sim 4000$  shots, respectively [12]. Therefore, it can be said that the deposition rate per shot was increased for 2013 experimental campaign. The H and D retentions were 2–3 times as large as that for 2012 experimental campaign. In LHD, high-temperature and steady-state operation experiments were conducted and remarkable progresses were reported [14–16]. These facts anticipate that the flux of hydrogen during the deposition of carbon based mixed-material layer can be enhanced and hydrogen isotope retention would be slightly increased, compared to that for 2012 experimental campaign, but H retention for DP sample would have reached almost saturation concentration and no large enhancement was found. However, more detail analysis will be required.

The behavior of He was also studied as shown in Fig. 8, and total He retention was summarized in Table 3 for the samples exposed in 2013. The He desorption was quite complex and several desorption peaks were found. For ER sample, the desorption was observed from lower temperature of 400 K and large desorption peak was located at 800 K. For the other samples, the desorption was initiated at  $\sim 600$  K and several desorption peaks were found at the temperature between 700–1000 K. Tokitani et al. [17] has reported He TDS spectra for SS-316 samples exposed to long-pulse He discharge in the 2013 experimental campaign [16]. The TDS spectra were quite consistent with our results, but our data was limited within the temperature up to 1173 K, but, according to Ref. [16], He desorption was extended more than 1300 K. As observed in TEM, the carbon based mixed-material deposition layer was quite porous and amorphous and most of He, especially for 48 min

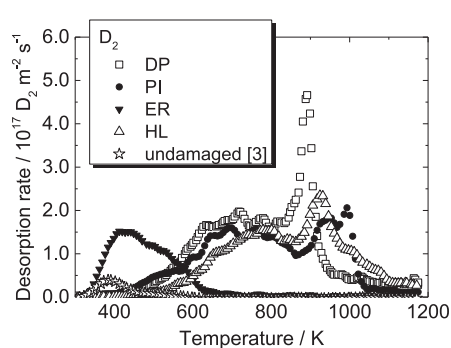
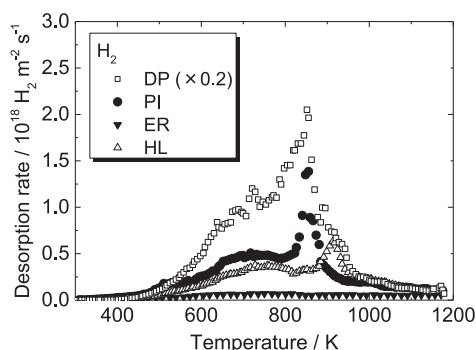


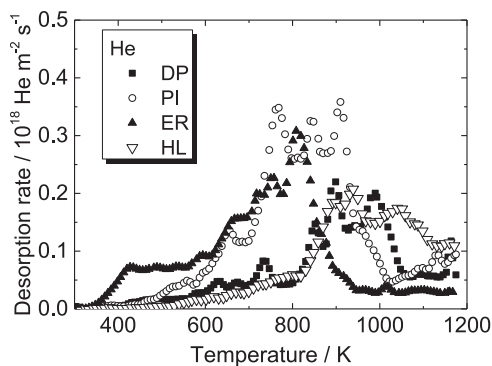
Fig. 6. H<sub>2</sub> and D<sub>2</sub> TDS spectra for deuterium ion implanted tungsten exposed to 2013 experimental campaign.



**Table 2**

Summary of H and D retentions for all the samples exposed to 2013 experimental campaign and thickness of mixed-material deposition layer.

Sample	2013 Campaign			2012 Campaign		
	Thickness ( $\mu\text{m}$ )	H retention ( $\text{H}/\text{m}^{-2}$ ) HD & $\text{H}_2$	D retention ( $\text{D}/\text{m}^{-2}$ ) HD & $\text{D}_2$	Thickness ( $\mu\text{m}$ )	H retention ( $\text{H}/\text{m}^{-2}$ ) HD & $\text{H}_2$	D retention ( $\text{D}/\text{m}^{-2}$ ) HD & $\text{D}_2$
DP	~5.0	$9.8 \times 10^{21}$	$7.3 \times 10^{20}$	6.0	$6.3 \times 10^{21}$	$1.8 \times 10^{20}$
PI	0.4	$1.7 \times 10^{21}$	$4.5 \times 10^{20}$	0.5	$7.9 \times 10^{20}$	$3.1 \times 10^{20}$
ER	~0	$5.2 \times 10^{20}$	$2.1 \times 10^{20}$	~0	$2.0 \times 10^{20}$	$6.4 \times 10^{19}$
HL	0.3	$1.2 \times 10^{21}$	$3.5 \times 10^{20}$	0.2	$4.8 \times 10^{20}$	$7.5 \times 10^{19}$

**Fig. 8.** He TDS spectra for deuterium ion implanted tungsten exposed to 2013 experimental campaign.**Table 3**Total He retention ( $\text{He m}^{-2}$ ) in the samples.

DP	PI	ER	HL
$1.1 \times 10^{20}$	$2.0 \times 10^{20}$	$1.6 \times 10^{20}$	$1.2 \times 10^{20}$

steady-state He discharge, would be quickly desorbed during the operation and He retention should be more than one order lower than hydrogen isotope retention.

These results indicate that hydrogen isotope retention was controlled by thickness of the carbon based mixed material layer, which consisted of carbon and the first wall materials of Fe, Cr and so on. Large amount of hydrogen isotope was retained in it except for erosion-dominated area (ER sample). For the steady-state operation, the control of wall pumping effect by this mixed material layer would be quite important. In addition, He steady-state operation introduces He bubbles and damages in this layer, but most of He was not retained in wall materials and He retention was almost 1/10 compared with hydrogen isotope retention even if the numbers of hydrogen shots and He shots are ~4600 shots and ~2500 shots, respectively. But, some of He would be trapped stably in both of bulk of metal and carbon based mixed material layer.

#### 4. Conclusions

Effect of carbon based mixed-material deposition layer formation on hydrogen isotope retention was studied. The W samples were exposed to ~4000 shots of H plasma in the 2013 plasma experimental campaign. Most of the sample surfaces except for ER were covered by a carbon based mixed-material deposition layer, which mainly consisted of carbon, but some of metal impurities like Fe, Cr and so on, were contained. The thick carbon based mixed-material deposition layer with ~5  $\mu\text{m}$  was found for the DP sample. For the ER sample, He bubble was formed due to long term He discharge during plasma experimental campaign. The additional 1 keV  $\text{D}_2^+$  implantation was performed to evaluate the

D retention enhancement by plasma exposure. It was found that H retention was controlled by the thickness of the carbon-dominated mixed-material deposition layer, indicating most of the H was uniformly trapped by this mixed-material deposition layer. It is concluded that the accumulation of low-Z mixed-material layer on the surface of first wall is one of key issues for the determination of hydrogen isotope retention in first wall and control of wall pumping effect.

#### Acknowledgments

This study has been supported by NIFS collaboration programs No. NIFS15K0BF033 & NIFS14KLEF013, University of Toyama Collaboration Program and Instrumental Research Support Office, Research Institute of Green Science and Technology at Shizuoka University.

#### References

- [1] Y. Ueda, H.T. Lee, N. Ohno, et al., Recent progress of tungsten R&D for fusion application in Japan, *Phys. Scr.* T145 (2011) 014029.
- [2] M. Rieth, S.L. Dudarev, S.M. Gonzalez de Vicente, et al., A brief summary of the progress on the EFDA tungsten materials program, *J. Nucl. Mater.* 442 (2013) S173–S180.
- [3] Y. Oya, X. Li, M. Sato, et al., Thermal desorption behavior of deuterium for 6 MeV Fe ion irradiated W with various damage concentrations, *J. Nucl. Mater.* 461 (2015) 336–340.
- [4] H. Fujita, K. Yuyama, X. Li, et al., Effect of neutron energy and fluence on deuterium retention behavior in neutron irradiated tungsten, *Phys. Scr.* T167 (2016) 014068.
- [5] Y. Oya, M. Shimada, M. Kobayashi, et al., Comparison of deuterium retention for ion-irradiated and neutron-irradiated tungsten, *Phys. Scr.* T145 (2011) 014050.
- [6] Y. Hatano, M. Shimada, Y. Oya, et al., Retention of Hydrogen isotopes in neutron irradiated tungsten, *Mat. Trans.* 54 (2013) 437–441.
- [7] Y. Hatano, M. Shimada, T. Otsuka, et al., Deuterium trapping at defects created with neutron and ion irradiations in tungsten, *Nucl. Fusion* 53 (2013) 073006.
- [8] V. Kh. Alimov, J. Roth, R.A. Causey, et al., Deuterium retention in tungsten exposed to low-energy, high-flux clean and carbon-seeded deuterium plasmas, *J. Nucl. Mater.* 375 (2008) 192–201.
- [9] S.K. Sharma, H. Zushi, N. Yoshida, et al., Analysis of PWI footprint traces and material damage on the first walls of the spherical tokamak QUEST, *Fusion Eng. Des.* 87 (2012) 77–86.
- [10] Y. Oya, S. Masuzaki, T. Fujishima, Enhancement of hydrogen isotope retention in tungsten exposed to LHD plasmas, *J. Nucl. Mater.* 438 (2013) S1055–S1058.
- [11] Y. Oya, S. Masuzaki, M. Tokitani, et al., Enhancement of hydrogen isotope retention capacity for the impurity deposited tungsten by long-term plasma exposure in LHD, *Fusion Eng. Des.* 88 (2013) 1699–1703.
- [12] Y. Oya, S. Masuzaki, M. Tokitani, et al., Comparison of hydrogen isotope retention for tungsten probes in LHD vacuum vessel during the experimental campaigns in 2011 and 2012, *Fusion Eng. Des.* 89 (2014) 1091–1095.
- [13] S. Masuzaki, et al., Design and installation of the closed helical divertor in LHD, *Fusion Eng. Des.* 85 (2010) 940–945.
- [14] H. Takahashi, High Ion temperature plasmas using an ICRF wall-conditioning technique in the LHD, *Plasma Fusion Res.* 9 (2014) 1402050.
- [15] K. Nagaoka, H. Takahashi, S. Murakami, Integrated discharge scenario for high-temperature helical plasma in LHD, *Nucl. Fusion* 55 (2015) 113020.
- [16] H. Kasahara, T. Seki, K. Saito, Development of steady-state operation using ion cyclotron heating in the large helical device, *Phys. Plasmas* 21 (2014) 061505.
- [17] M. Tokitani, H. Kasahara, S. Masuzaki, et al., Plasma wall interaction in long-pulse helium discharge in LHD – Microscopic modification of the wall surface and its impact on particle balance and impurity generation, *J. Nucl. Mater.* 463 (2015) 91–98.